

Ultrafast spin dynamics: role of laser-induced modification of exchange parameters

Sergiy Mankovsky,¹ Svitlana Polesya,¹ and Hubert Ebert¹

¹*Department of Chemistry/Phys. Chemistry, LMU Munich,
Butenandtstrasse 11, D-81377 Munich, Germany*

(Dated: April 29, 2024)

Induced by an ultra-short laser pulse, the electronic structure of a material undergoes strong modifications leading to a fast demagnetization in magnetic materials. Induced spin-flip transitions are one of the reasons for demagnetization, that is discussed in the literature as a Stoner-like mechanism. On the other hand, demagnetization due to transverse spin fluctuations is usually discussed on the basis of the Heisenberg Hamiltonian and hardly accounts for the modification of the electronic structure. In this work we demonstrate a strong impact of the laser-induced electron transitions, both spin-flip and spin-conserving, on the exchange coupling parameters. For this, a simple two-step scheme is suggested. As a first step, the electronic structure time evolution during the ultra-short laser pulse is described accurately within time-dependent density-functional theory (TD-DFT) calculations. As a next step, the information on the time-dependent electronic structure is used for calculations of the parameters of the Heisenberg Hamiltonian. A strong modification of the exchange coupling parameters is found in response to the applied ultra-short laser pulse. The most important reason for this modification is played by the laser induced repopulation of the electronic states. Although the changes of the exchange parameters are most prominent during the laser pulse, they may be important also for the magnetic relaxation. The same concerns the spin-lattice interactions playing a central role for the relaxation process. A strong impact of the laser-induced modification of the electronic structure on the spin-lattice coupling parameters is also shown in this work.

I. INTRODUCTION

Ultrafast spin manipulation is one of the most exciting research topics in the latest decades. Since the first report by Beaurepaire et al.¹, demonstrating that magnetic order can be manipulated on a sub-picosecond timescale using ultrashort laser pulses, many efforts have been done, both experimental and theoretical, to shed light on the physical processes behind ultrafast magnetic dynamics on the one hand side and to adjust these processes to control, e.g. the magnetization dynamics in magnetic materials²⁻⁴. Despite the huge progress made by these activities, the various microscopic mechanisms responsible for the demagnetization at different time scales is still under debate.^{1,5-9} Definitely, one can see a consensus in the literature concerning the role of the spin-orbit coupling (SOC) responsible for the laser-induced demagnetization in metals leading to an angular momentum transfer from the spin subsystem to other degrees of freedom^{6,10} via spin-flip transitions during the laser field induced excitation^{10,11} or Elliott-Yafet-like processes with spin-flip electron scattering on phonons^{7,12-14}. The Stoner-type demagnetization mechanism is described reasonably well within time dependent density functional theory (TD-DFT)^{15,16}. It should be stressed that such calculations are usually performed for a non-distorted crystal lattice and a collinear magnetic state. On the other hand, the impact of the electron-phonon scattering on the time evolution of the magnetization was reported recently¹⁶ by performing TD-DFT calculations in the presence of preexcited phonon modes in the system. Apart from TD-DFT, other quantum-mechanical investigations have been done estimating the

rate of angular momentum transfer from the electron to the lattice and magnetic degrees of freedom via SOC-driven spin-flip electron scattering^{6,7,9,13,17,18}.

The experimental observation of a strong laser-induced magnetization decay observed by Eich et al.¹⁹ in Co led the authors to the conclusion, that the ferromagnetic-paramagnetic phase transition is a result of an extremely efficient ultrafast generation of collective transverse spin excitations, i.e. magnons, rather than a loss of the exchange splitting. Tengdin et al.²⁰, also report about the demagnetization in Ni which occurs much earlier than the collapse of the exchange splitting. The authors, however, suggest that the ultrafast demagnetization is driven by a highly nonequilibrium process, e.g. superdiffusive spin currents.

Attributing the ultrafast demagnetization to magnetic disorder in a ferromagnet, a natural question is what is the efficient mechanism responsible for ultrafast generation of magnons, which will depend on the material. To find the answer to this question, an efficient way is to combine classical models used for spin dynamics with first-principles DFT calculations. This may be for instance the atomistic Landau-Lifshitz-Gilbert (LLG) model based on a classical spin Hamiltonian²¹ giving access to the magnetic torque accounting for contributions from isotropic exchange, Dzyaloshinskii-Moriya interactions (DMI), and magnetic anisotropy calculated from first principles²². The ab-initio parametrized quantum kinetic approach was reported recently to describe magnon occupation dynamics due to electron-magnon scattering in ferromagnetic metals excited by ultrafast laser radiation²³. The results demonstrate a strong demagnetization of Fe within 200 fs due to an ultrafast generation of high-energy magnons. The optically induced

magnetic torque may be a consequence of a coupling between the electric field of the laser light and the electron spins^{24–29}, and may originate, e.g., due to the optical spin transfer torque^{24,30} or due to the inverse Faraday effect (IFE)^{25–29}. Furthermore, it may be seen as a consequence of the optically-induced changes of the interatomic exchange interactions^{25,26}. The laser induced demagnetization and relaxation may also be controlled by spin-lattice interactions, which are responsible for the angular momentum transfer between the magnetic subsystem and the crystal lattice leading to ultrafast magnon or phonon generation in the demagnetization and relaxation processes, respectively^{8,31,32}.

One should note, however, that the efficiency of the magnon generation should depend not only on the mechanism of magnon excitation, but also on the properties of the magnon spectrum determined by the parameters of the spin Hamiltonian. Ultrafast heating of the electronic subsystem should almost immediately (i.e. on the time scale of $\sim 10^{-15}$ s) result in a modification of all parameters entering the equations used to describe spin-dynamics. Accordingly, all parameters should change with time following the absorbed energy and corresponding time evolution of the electronic subsystem. This concerns, in particular, the anisotropy field generated due to the absorbed laser pulse³³. In general, the theoretical description of these changes for the non-equilibrium electron density require to go beyond the standard approach used for the equilibrium, and should rely, for instance, on the non-equilibrium Green's-function formalism^{27,34}, or exact diagonalization approach³⁵. Alternatively, we suggest in the present work a simple scheme to demonstrate the impact of the optically excited out-of-equilibrium electron subsystem on the demagnetization or relaxation processes. Information about the laser-pulse excited electron system is obtained via TD-DFT calculations, which are used here to determine the time evolution of the exchange coupling and spin-lattice coupling parameters. As a result, the spin dynamic characteristics should follow the changes of all the parameters that determine the torque on the magnetic moments.

Note that on a longer time scale, when the magnetization is also decreased due to increasing magnetic disorder, its impact on the exchange coupling parameters may be significant and should also be taken into account²².

II. RESULTS AND DISCUSSION

A. Magnetic torque due to the optical heating of the electronic subsystem

We focus first on the impact of the transverse spin fluctuations on the laser-induced demagnetization in ferromagnets. When the system is in equilibrium, these fluctuations are reasonably well described using the extended Heisenberg spin model Hamiltonian $\mathcal{H}_{\text{Heis}}$ with the parameters calculated from first principles, i.e. the pa-

rameters representing symmetric exchange interactions, Dzyaloshinskii-Moriya interactions, magnetic anisotropy, etc. The spin evolution out of equilibrium described by the atomistic Landau-Lifshitz-Gilbert equation³⁶, is governed by the torque on the magnetic moments on the sites i , $\vec{T}_i = \hat{s}_i \times \vec{H}_{\text{eff},i}$. The torque is determined by the external perturbation field and effective magnetic field, $\vec{H}_{\text{eff},i} = -\frac{\partial \mathcal{H}}{\partial \hat{s}_i}$, given in particular, in terms of the spin Hamiltonian $\mathcal{H} = \mathcal{H}_{\text{Heis}}$.

For a system affected by an ultrafast laser pulse, one can consider the magnetic torque $\Delta \vec{T}_{\text{Heis},i}$ created due to changes of the parameters of the model Hamiltonian, i.e. $\Delta J_{ij}(t)$ and $\Delta \vec{D}_{ij}(t)$, $\Delta \underline{K}_i(t)$ as a result of the strong laser-induced heating of the electron subsystem. Note that in general, the torque on the magnetic moment should account for the impact of the spin evolution during the whole time period starting with the laser pulse (see, e.g. Ref. [36]). However, using a simplified time-dependence for the magnetic torque, one can derive it from the current state of the electronic structure evolving in time. Despite the resulting uncertainty of the numerical results, this allows a qualitative, semi-quantitative, analysis of the impact of the laser-excited electronic subsystem on the transverse spin dynamics.

Considering bcc Fe with a non-distorted crystal lattice ($T_{\text{lat}} = 0$ K) as an example, we will focus on the laser induced changes of the isotropic exchange interactions represented by the parameter $\Delta J_{ij}(t)$ and the corresponding magnetic torque $\Delta \vec{T}_i = \sum_j (\hat{s}_i \times \hat{s}_j) \Delta J_{ij}$, while the DMI parameters should vanish because of the inversion symmetry. Furthermore, the parameters of the magnetocrystalline anisotropy (MCA) are very weak in the bulk.

The torque determined this way, however, does not give access to the angular momentum transfer to the spin subsystem resulting in the generation of new magnons responsible for the transverse demagnetization. As discussed above, magnon generation can be driven by the optically induced magnetic torques that stem from the direct laser light interaction with the magnetic moments²⁶, or from the phonon-magnon scattering. The latter mechanism is determined by spin-lattice coupling (SLC) DMI-like, $\vec{D}_{ij,k}^\mu$, and MCA-like, $\underline{K}_{i,k}^\mu$ parameters^{37,38} entering the spin-lattice Hamiltonian \mathcal{H}_{sl} (see Appendix B), and require a finite temperature of the lattice subsystem leading to a broken local symmetry at the atomic sites due to a finite amplitude of the lattice fluctuations. As a consequence, magnetic torques created by the effective fields $H_{\text{sl},i}^\alpha = -\frac{\partial \mathcal{H}_{\text{sl}}}{\partial s_i^\alpha}$ ^{31,37,38} may change in the case of a strong laser-induced excitation of the electronic subsystem, leading to a corresponding induced torque $\Delta \vec{T}_{\text{sl},i}(t)$ determined by the change of the SLC parameters following the time evolution of the excited electronic system.

In order to demonstrate the impact of such a modification of the exchange coupling parameters, we consider the system at a certain time step instead of performing an integration of the atomistic equations of motion.

The electronic structure for any time step found within a TD-DFT calculations (here using the Elk code³⁹) can be used later on to calculate the exchange coupling parameters for this time step. We focus in this work on two types of changes in the electronic subsystem, the spin-dependent part of the electronic potential (in particular, the exchange field $B_{xc} = \frac{1}{2}(V^\uparrow - V^\downarrow)$) and the re-population of the electronic states, which in our opinion has the main impact on the exchange parameters. The goal is to demonstrate a significant role of the laser induced modifications of these parameters for spin dynamics, in particular for laser-induced demagnetization

dynamics.

To account for the re-population when calculating the exchange parameters, one has to adopt the expression for the exchange coupling parameters worked out previously^{40–42} for the case of a reasonably low temperatures ($\lesssim T_C$), when the Fermi-Dirac occupation function $f(E)$ can be well approximated by the step function. Taking into account the temperature or laser-pulse induced modifications of $\underline{f}(E)$ which become significant in the high temperature (or strong pulse fluence) regime, one obtains an expression for the elements of the \underline{J}_{ij} tensor as follows (see Appendix A)

$$J_{ij}^{\alpha\beta} = -\frac{1}{2} \left[\frac{1}{\pi} \text{ImTr} \int_{-\infty}^{\infty} dE \frac{d\underline{f}(E)}{dE} (E - \mu(T)) \langle \Delta V \rangle_i^\alpha \underline{\tau}_{ij}(E) \langle \Delta V \rangle_j^\beta \underline{\tau}_{ji}(E) + \frac{1}{\pi} \text{ImTr} \int_{-\infty}^{\infty} dE \underline{f}(E) \langle \Delta V \rangle_i^\alpha \underline{\tau}_{ij}(E) \langle \Delta V \rangle_j^\beta \underline{\tau}_{ji}(E) \right], \quad (1)$$

with $\underline{f}(E)$ the spin-dependent occupation function. A similar expression can be derived also for the spin-lattice parameters. However, below we focus on the properties of the isotropic exchange coupling parameters, $J_{ij} = \frac{1}{2}(J_{ij}^{xx} + J_{ij}^{yy})$, and the DMI-like SLC parameters.

B. Exchange coupling parameters for out of equilibrium situation

As a first step we consider the system being at a finite temperature T . This allows us to simulate the effect of the optically induced re-population of the electronic states, which can be seen as a heating of the electronic structure to a temperature in the order of 10^4 K (see below). The resulting impact for the heated electronic subsystem with temperature T_{el} is described by the corresponding Fermi-Dirac distribution function. In contrast to this, we do not account for any changes of the electron potential, as well as thermal atomic displacements and a deviation of the spin moments from perfect FM ordering, i.e., we neglect at the moment their impact on the exchange parameters. This simplification allows to demonstrate the impact of the heated electronic subsystem on the magnetic properties of the system in the thermal equilibrium represented by the Heisenberg model.

The parameters J_{ij} calculated for bcc Fe for five different temperatures are represented in Fig. 1. We focus here only on these parameters, first of all because they are responsible for the FM order and characterize the Curie temperature in the system, while the DMI parameters are equal to zero for symmetry reason.

The top panel in Fig. 1 shows the temperature dependent Fermi function $f(E, T_{el})$ for the temperatures (a) 0 K, (b) 3000 K, (c) 6000 K, (d) 9000 K, and (e) 12000 K. The corresponding exchange coupling param-

eters J_{ij} for bcc Fe are shown in the bottom panel. One can clearly see their significant decrease with increasing electronic temperature. This in turn should lead to a decrease of the Curie temperature, as can be demonstrated by Monte Carlo simulations for a finite temperature T_{Heis} of the spin subsystem. It is worth noting that this implies thermalization of the spin subsystem, that occurs at the timescale of $\sim 10^{-12}$ s, i.e. much longer than the duration of a typical laser pulse considered here^{2,4}. This point has to be discussed in addition, when dealing with a realistic situation.

To get more insight into the behavior of the J_{ij} parameters, Fig. 2(a) shows the energy dependence of the integrand in the second term of Eq. (1) which determines the interatomic nearest-neighbor (nn) and next-to-nearest-neighbor (nnn) exchange coupling parameters J_{01} and J_{02} , respectively, for bcc Fe in the ground state, i.e. $T = 0$ K. Note that the first term in Eq. (1) vanishes in this case because of the distribution function $f(E, T_{el} = 0) = \theta(E - E_F)$. For both curves in Fig. 2(a), one can see a pronounced variation in the energy region close to the Fermi energy. The corresponding integrals in Eq. (1), using the energy E_{occ} as an upper limit of integration, represent the parameters $J_{01}(E_{occ})$ and $J_{02}(E_{occ})$ as a function of occupation of the electronic states. As can be seen in Fig. 2(b), these parameters exhibit a strong dependence on the occupation of the electronic states (see, e.g., discussions in Ref. [43]). A crucial consequence of the strong energy dependencies shown in Fig. 2(a) occurs for the out-of-equilibrium electron subsystem with the laser-induced deoccupied states below E_F , and occupied states above E_F . In this case the main changes of the exchange parameters occur as a result of a convolution of the integrand plotted in Fig. 2(a) with the occupation function $f(E)$ shown in Fig. 4. This can be seen in Fig. 2(b), dashed line, representing the

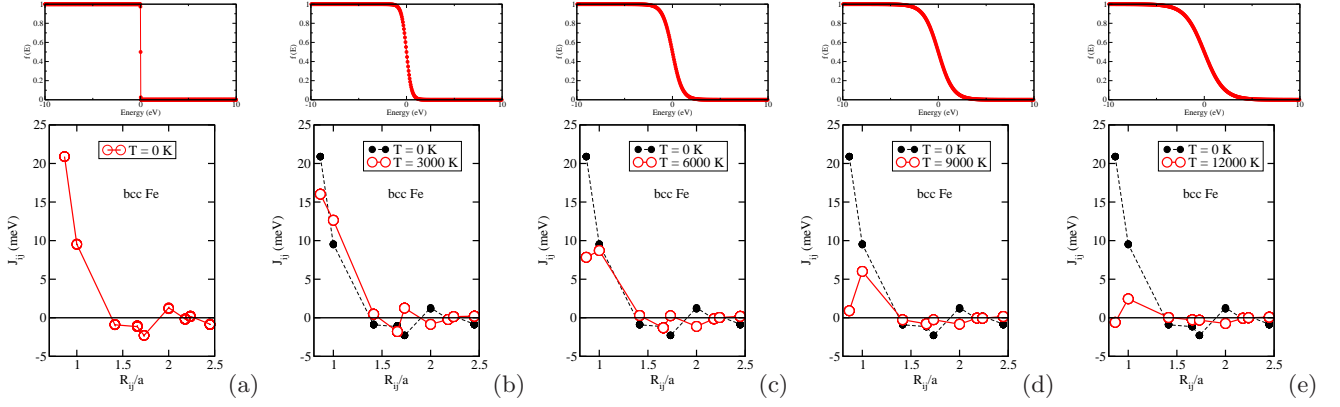


FIG. 1. The Fermi-Dirac distribution corresponding to temperatures (a) 0 K, (b) 3000 K, (c) 6000 K, (d) 9000 K, (e) 12000 K, together with corresponding results for the temperature dependent exchange coupling parameters $J_{ij}(T)$ for bcc Fe.

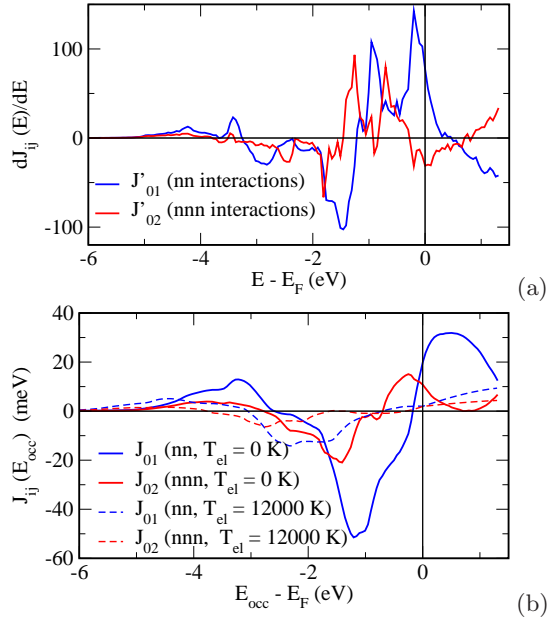


FIG. 2. (a) The integrand in the second term of Eq. (1) for the interatomic nn and nnn exchange coupling parameters of bcc Fe in the ground state ($T_{el} = 0$ K) as a function of energy; (b) interatomic nn and nnn exchange coupling parameters, J_{01} and J_{02} , respectively, represented as a function of occupation of the electronic states characterized by the threshold energy E_{occ} below or above the Fermi energy E_F . Solid lines represent results obtained for the electronic temperature $T_{el} = 0$ K, while dashed lines correspond to $T_{el} = 12000$ K.

$J_{01}(E_{occ}, T)$ and $J_{02}(E_{occ}, T)$ parameters obtained using the occupation function $f(E, T_{el} = 12000K)$ (see Fig. 1).

C. Exchange coupling parameters under laser pulse and ultrafast demagnetization

As a next step, we focus on the magnetic properties of a material determined by laser induced changes of

the exchange interactions, considering also bcc Fe as an example and making use of Eq. (1). In this case we use as an input the exchange field $B_{xc} = \frac{1}{2}(V^\uparrow - V^\downarrow)$ and spin-resolved occupation function $f_\sigma(E)$, delivered by TD-DFT calculations performed with the Elk electronic structure code³⁹, for a laser pulse polarized along the x axis, a fluence of 24 mJ/cm², a frequency of 413 THz and full width at half maximum (FWHM) of 4.8 fs. The TD-DFT calculations have been performed for the

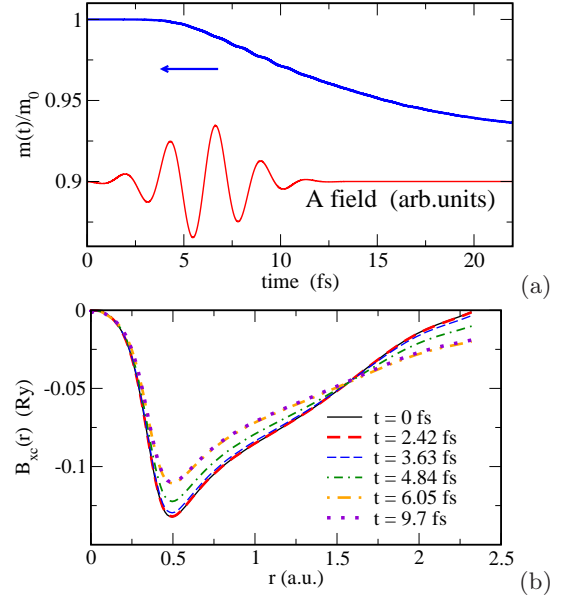


FIG. 3. (a) Laser-pulse induced magnetization for bcc Fe. TD-DFT calculations using a laser pulse polarized along the x axis, fluence 24 mJ/cm², FWHM of 4.8 fs. (b) Radial dependence of the effective exchange field $B_{xc}(r) = \frac{1}{2}(V^\uparrow - V^\downarrow)$ for Fe within the muffin-tin sphere, plotted for different time steps during the laser pulse.

time interval up to 22 fs. As one can see in Fig. 3 (a), the magnetization decreases during the laser pulse by $\sim 4\%$ due to the SOC-induced spin-flip transitions. It continues to decrease also after the laser pulse down to $\sim 8\%$, due

to the relaxation within the electronic subsystem accompanied by SOC-induced spin-flip transitions between the 'up' and 'down' spin channels characterized by different out-of-equilibrium occupation functions $f_\sigma(E, t)$.

The decrease of the Fe magnetic moment is a consequence of the modified spin density due to the repopulation of the electronic states, induced by the laser pulse. This in particular results in a change of the effective exchange field $B_{xc}(r)$ shown in Fig. 3 (b), plotted within the muffin-tin sphere for different time steps. One can clearly see a decrease of the magnitude of the B-field during the laser pulse, while the changes are almost invisible when the pulse is finished.

The laser-induced spin-dependent occupation function $f_\sigma(E, t)$ plotted in Fig. 4, top panel, is represented for five time steps during the laser pulse. One can see a considerable depopulation of the electronic states below E_F due to the optical excitation to high-energy states. Moreover, in contrast to finite-temperature considerations discussed above, the occupation functions are different for the majority- and minority-spin states, and the difference increases during the laser pulse.

The quantities $B_{xc}(r)$ and $f_\sigma(E, t)$ have been used in a quasi-stroboscopic way for calculations of the Green function varying in time under the influence of the laser pulse, to be used later on for calculation of time-dependent exchange coupling parameters. The calculations have been performed by means of the SPR-KKR band structure method using $B_{xc}(r)$ at every time step to calculate the corresponding scattering path operator and the perturbation potential $\langle \Delta V \rangle_i^\alpha$. The exchange coupling parameters, J_{ij} , modified under the impact of the laser pulse are given in the middle panel of Fig. 4. As one would expect, the J_{ij} parameters decrease with time during the laser pulse. The most pronounced changes concern the nearest-neighbor and next-nearest-neighbor parameters. After the pulse, the exchange parameters remain practically unchanged (see Fig. 4(e), middle panel).

To illustrate, which impact on the magnetic properties can be expected due to such a modification of the exchange interactions, one can consider the system at every time step as one being electronically in a frozen state. As can be seen in Fig. 4 (bottom), the modification of the exchange interactions shown in Fig. 4 (middle) leads to a softening of the magnon spectrum, reflecting the fact that the magnetization gets less robust. In line with this, we find a distinct decrease of the effective Curie temperature during the absorption of the laser pulse (see Fig. 5(a)), which was obtained from Monte Carlo simulations using the fixed exchange coupling parameters. Furthermore, considering the initial temperature for the spin subsystem, T_{Heis} , to be finite and fixed during the laser pulse, which seems to be a reasonable approximation for the ultrashort time scale, one can check the time dependent behavior of the net magnetization using different exchange parameters calculated for different time steps. Corresponding results for the magnetization evolution obtained making use of the parameters shown in

Fig. 4 are plotted in Fig. 5(b) for three different temperatures T_{Heis} , demonstrating a strong magnetization decrease during the laser pulse which can lead even to the break of the magnetic order if T_{Heis} is high enough. Obviously, these conclusions on the magnetic properties have essentially semi-qualitative character because of the approximations discussed above. Nevertheless, we would like to stress that they are based on the electronic structure with its time evolution coherently treated within the TD-DFT formalism.

In a more realistic scenario, T_{Heis} is non-zero and can change also during and after the laser pulse, that happens however on a longer time scale. This implies a magnetic disorder in the system varying in time until the full relaxation of the excited system. As the exchange parameters depend also on the magnetic configuration, this situation can also be taken into account considering the laser induced demagnetization and relaxation processes. Such investigations have been performed recently combining first principles calculations and spin dynamics simulations²², where the finite temperature effect after the laser pulse has been taken into account for the electron and spin subsystems. However, in that work, both effects were small because of a weak laser power used in the calculations (for comparison, the maximal effective temperature of the electron gas considered in this work was about 1000 K, far below the effective temperature $\sim 10^4$ K estimated for the laser pulse used in the present case.) Furthermore, the thermalization of the spin and lattice subsystems at later times results in an increase of the magnetic disorder as well as increase of the amplitude of atomic displacements. One can compare the impact of these factors on the exchange coupling with the impact of the laser-induced strong excitation of the electron subsystem. For this we consider the limiting case of $T = T_C$ with thermally induced magnetic disorder treated here making use of the relativistic disordered local moment (RDLM) theory^{44,45}. Corresponding exchange coupling parameters J_{ij} are plotted by squares in Fig. 6. As one can see, the nnn parameters decrease significantly when compared to the FM system ($T = 0\text{K}$), however at the same time one can see an increase of the nn parameters. Obviously, this effect is very different when compared to the effect caused by the laser-excited out-of-equilibrium electron subsystem. The lattice vibrations at this temperature⁴³ also lead to some changes of J_{ij} , which however mainly concern the nn parameters.

D. Spin-lattice coupling parameters

Finally we will shortly discuss another type of interaction, namely the spin-lattice interactions responsible for the energy and angular momentum transfer between the magnon and phonon subsystems. These interactions are discussed, in particular, for a long time scale when considering the mechanisms responsible for the magnetic relaxation³⁷.

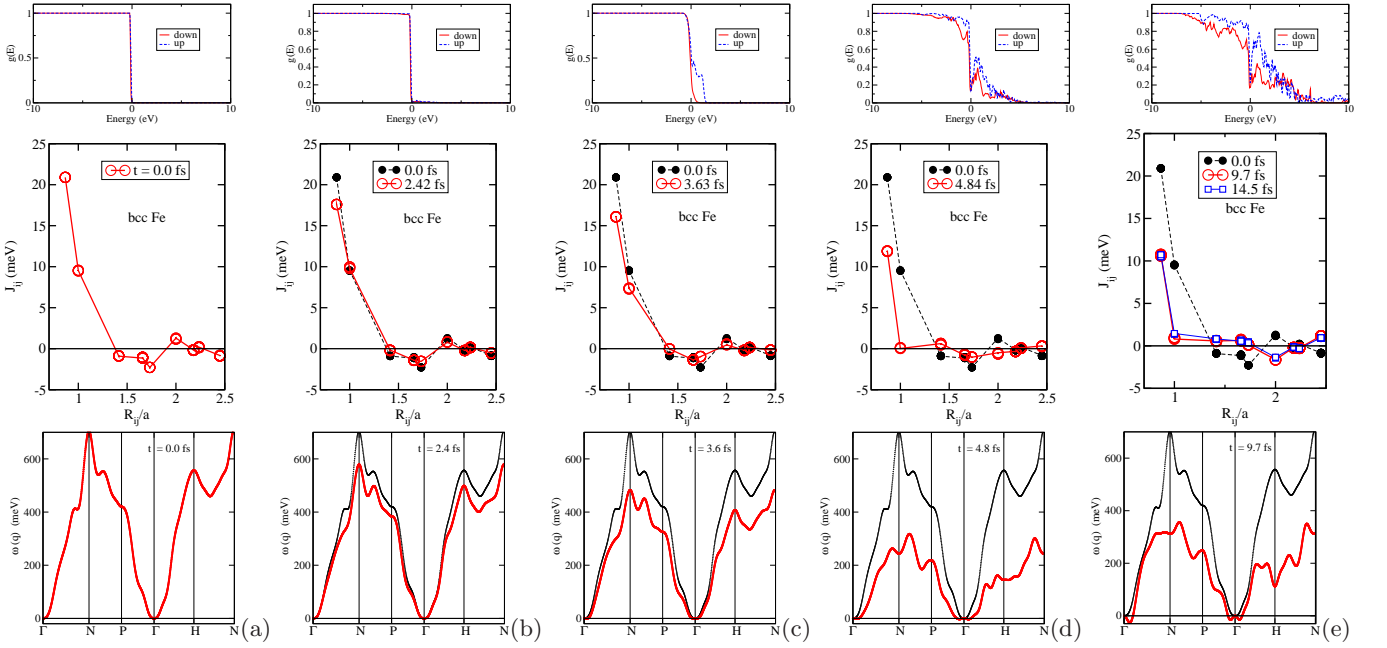


FIG. 4. (Top) spin-dependent electronic occupation function $f_{\sigma}(E, t)$ for five time steps during the laser pulse, calculated using the Elk TD-DFT code, with the laser pulses parameters: FWHM = 4.8 fs, pulse fluence of 24 mJ/cm², light frequency 413 THz. (Middle) The exchange coupling parameters J_{ij} (open symbols) calculated for several time steps with the SPR-KKR band structure code using corresponding occupation functions $f_{\sigma}(E, t)$ (top panel) and effective exchange field B_{xc} obtained within TD-DFT calculations. Full symbols represent the results for the ground state parameters. (Bottom) Spin-wave dispersion relations calculated for different time steps (red symbols) using the exchange parameters shown in the middle panel. Black symbols represent the results for the ground state.

The impact of the lattice vibrations on the exchange coupling parameters is demonstrated in Fig. 6. Discussing this in terms of the spin-lattice interaction, it was shown³⁸ that it can be associated with the SLC parameters of second order with respect to displacements, $J_{ij,kl}^{\alpha\alpha,\mu\nu}$, leading to corrections of the exchange coupling $\Delta J_{ij} \sim \langle u^2 \rangle_T$. Note that the amplitude of the atomic displacement is directly connected to the lattice temperature T_{lat} , and can be reasonably well estimated for a given temperature T_{lat} within the Debye model approach. A more pronounced effect is expected due to the SLC parameters linear w.r.t. the atomic displacements. These parameters characterize the rate of spin angular momentum transfer due to the torque on the magnetic moments, $\vec{T}_i = \hat{e}_i \times \vec{H}_{\text{eff}}$, caused by the effective field induced by the displacements u_k^{μ} of the atoms on sites k , or alternatively, due to the mechanical torque on the atom k , $\vec{\Sigma}_k^{ph} = \vec{u}_k \times \vec{F}_k$, created by the forces induced by spin tiltings \hat{e}_i^{α} on sites i ^{31,37,38}.

Similar to the exchange coupling parameters, the SLC parameters are determined by the electronic structure and one can expect their changes caused by the laser induced strong modification of the electron subsystem. We will focus here only on the so-called DMI-like SLC parameters $\vec{D}_{ij,k}^{\mu}$ ^{37,38}, characterizing the change of the DMI parameters $\Delta \vec{D}_{ij} = \sum_{k,\mu} \vec{D}_{ij,k}^{\mu} (u_k^{\mu} - u_i^{\mu})$ caused by atomic displacements \vec{u}_k (note that similar arguments

hold also when considering the properties of the MCA-like SLC parameters, $\mathcal{K}_{i,k}^{\alpha z, \mu}$ characterizing local changes of the MCA parameters $\Delta K_i^{\alpha z} = \sum_{k,\mu} \mathcal{K}_{i,k}^{\alpha z, \mu} (u_k^{\mu} - u_i^{\mu})$).

As an example, Fig. 7 shows the parameters $\mathcal{D}_{ij,j}^{z,\mu} u_D(T)$ represented as a function of time for three different temperatures of the crystal lattice T_{lat} : 300 K, 600 K and 1040 K. The lattice temperature is assumed to be constant during the full time range. One can see, that the SLC parameters (and corresponding contributions to $D_{ij}^{z,\mu}$) are of the order of 0.1 meV in the equilibrium, and change in amplitude and sign during the laser pulse reaching a value up to ~ 0.4 meV (depending on the lattice temperature). Similar arguments as in the case of the exchange coupling parameters may be used also to explain the time dependent change of the $\mathcal{D}_{ij,j}^{z,\mu}$ parameters. This is a consequence the strong energy dependent changes of the integrand (see Fig. 7(b)) in the expression for the SLC parameter (see Refs. [37 and 38]), leading in particular to a strong dependence of the SLC on the occupation of the electron states shown in Fig. 7(c).

III. SUMMARY

In summary, we find a distinct impact of the optically overheated electron subsystem on the inter-atomic exchange coupling parameters. While a simplified scheme

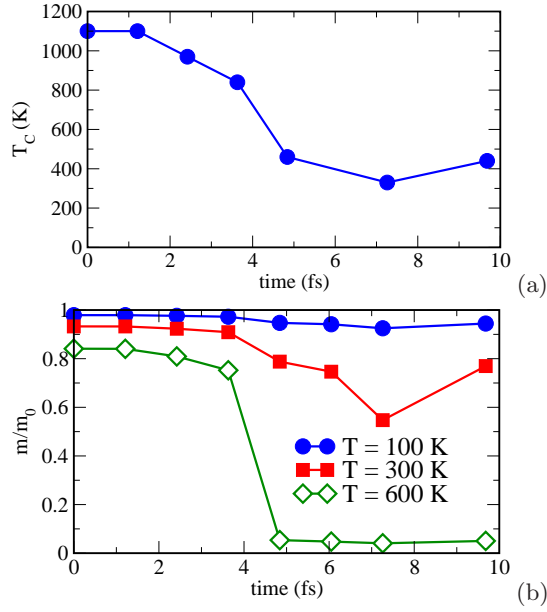


FIG. 5. (a) Curie temperature for bcc Fe as a function of time calculated using the exchange coupling parameters changing in time due to the laser pulse induced evolution of the electronic structure. (b) Time-dependent evolution of the magnetization for different temperature of the spin subsystem taken unchanged at the time interval shown in the plot. Even neglecting the energy transfer from the electronic subsystem in the ultrafast regime, the temperature can be seen as an initial temperature of the sample being in thermodynamic equilibrium.

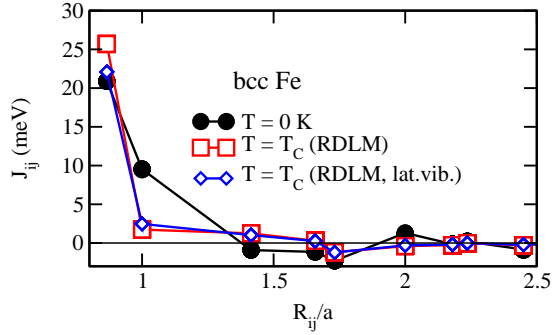


FIG. 6. Exchange coupling parameters J_{ij} for bcc Fe calculated for the FM reference state (full circles), for the magnetically disordered states treated within the RDLM approach (opened squares) and accounting both magnetic disorder and atomic diplacements at $T = T_C$. The amplitude of the lattice vibrations at given temperature is estimated using the Debye model^{43,45}.

is used to demonstrate this effect, the calculations of the exchange parameters rely on the electronic structure calculated using the TD-DFT method which ensure an accurate description of the electronic structure modifications under the influence of an ultrafast laser pulse. We have demonstrated a crucial role of the laser-induced de-occupation of the electronic states varying in time and

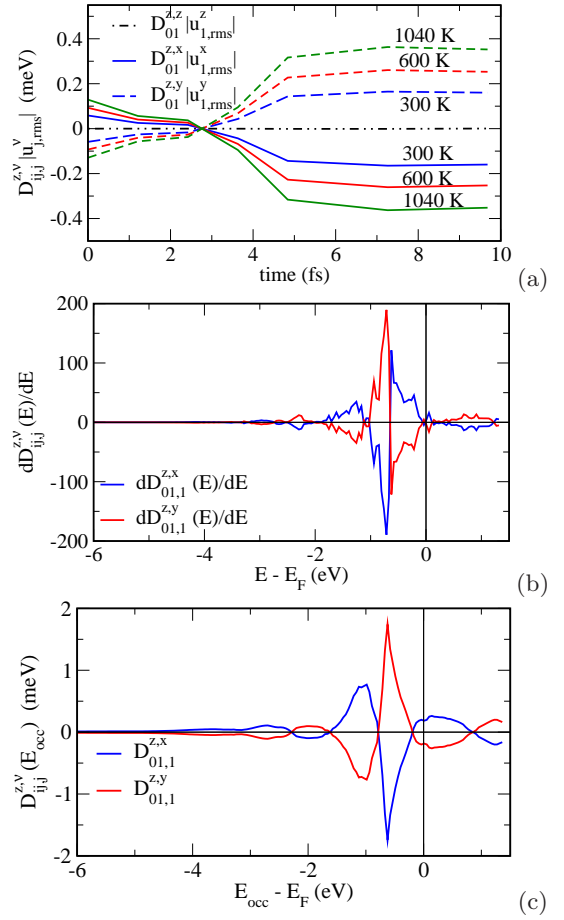


FIG. 7. (a) DMI-like spin-lattice coupling parameters as a function of time, represented by a contribution to the DMI parameters due to atomic displacement, $\mathcal{D}_{01,1}^{z,\mu}(u_j^\mu - u_i^\mu)$ for $\mu = x, y, z$ characterizing the directions of displacements of the atom in the position $\vec{R}_{01} = (-0.5, -0.5, -0.5)a_{lat}$. The results are presented for three different temperatures of the crystal lattice, 300 K, 600 K and 1040 K (T_C), described by the displacement amplitude given by rms displacement $u_D(T)$ estimated within the Debye model, i.e. 0.18, 0.28 and 0.39 a.u., respectively. (b) The integrands for the components of the DMI-like spin-lattice coupling parameters, $\mathcal{D}_{01,1}^{z,x}$ and $\mathcal{D}_{01,1}^{z,y}$, as a function of energy. (c) The components of the DMI-like spin-lattice coupling parameters, $\mathcal{D}_{01,1}^{z,x}$ and $\mathcal{D}_{01,1}^{z,y}$, represented as a function of occupation of the electronic states characterized by the threshold energy E_{occ} below or above the Fermi energy E_F .

dependent on the power of the laser pulse, leading to a strong weakening of the exchange parameters. Similarly, the laser-induced changes of the spin-lattice parameters can influence the efficiency of magnon generation and in turn the rate of demagnetization. At a longer time scale the laser-induced changes of the exchange parameters as well as spin-lattice parameters can influence the magnetization relaxation process and should correct the results obtained so far using equilibrium parameters.

IV. APPENDIX

In the presence of a perturbation, the Green function is modified as follows

Appendix A: Exchange coupling parameters out of equilibrium: impact of non-equilibrium occupation

Considering the FM state as a reference state, the deviation of some magnetic moments from the collinear FM state is described by the perturbation potential

$$\begin{aligned}\Delta V(\vec{r}) &= \sum_i \delta v(\vec{r} - \vec{R}_i) \\ &= - \sum_i \beta(\vec{\sigma} \cdot \delta \hat{m}_i) B_i^{xc}(r). \quad (\text{A1})\end{aligned}$$

$$G = G_0 + G_0 \Delta V G_0 + G_0 \Delta V G_0 \delta V G_0 + \dots = G_0 + \Delta G.$$

Accounting only for single particle contribution to the free energy, omitting the \vec{r} arguments, the perturbation results in a free energy change

$$\Delta F = \left(-\frac{1}{\pi}\right) \text{ImTrace} \int_{E_{\text{bottom}}}^{\infty} dE f(E) (E - E_F) \Delta G(E). \quad (\text{A2})$$

Keeping the second-order free energy term, one can use the sum rule for the Green functions $\frac{dG(E)}{dE} = -G(E)G(E)$ to transform this expression and taking into account the property of invariance of the trace under cyclic permutations of matrices, the expression above can be transformed as follows

$$\begin{aligned}\mathcal{F}^{(2)} &= \left(-\frac{1}{\pi}\right) \text{ImTrace} \int_{E_{\text{bottom}}}^{\infty} dE f(E) (E - E_F) G_0(E) \Delta V G_0(E) \Delta V G_0(E) \\ &= \left(\frac{1}{\pi}\right) \text{ImTrace} \int_{E_{\text{bottom}}}^{\infty} dE f(E) (E - E_F) \Delta V G_0(E) \Delta V \frac{d}{dE} G_0(E).\end{aligned} \quad (\text{A3})$$

By performing then the integration by parts, we arrive at

$$\begin{aligned}\mathcal{F}^{(2)} &= -\frac{1}{2} \left[\left(\frac{1}{\pi}\right) \text{ImTr} \int_{E_{\text{bottom}}}^{\infty} dE \frac{df(E)}{dE} (E - E_F) \Delta V G_0(E) \Delta V G_0(E) \right. \\ &\quad \left. + \left(\frac{1}{\pi}\right) \text{ImTr} \int_{E_{\text{bottom}}}^{\infty} dE f(E) \Delta V G_0(E) \Delta V G_0(E) \right].\end{aligned} \quad (\text{A4})$$

The first term should vanish for the ground state as $\frac{df(E)}{dE} = \delta(E - E_F)$.

Using the real space multiple scattering representation of the Green function $G_0(\vec{r}, \vec{r}', E)$

$$\begin{aligned}G(\vec{r}, \vec{r}', E) &= \sum_{\Lambda_1 \Lambda_2} Z_{\Lambda_1}^n(\vec{r}, E) \tau_{\Lambda_1 \Lambda_2}^{nn'}(E) Z_{\Lambda_2}^{n' \times}(\vec{r}', E) - \sum_{\Lambda_1} \left[Z_{\Lambda_1}^n(\vec{r}, E) J_{\Lambda_1}^{n \times}(\vec{r}', E) \Theta(r' - r) \right. \\ &\quad \left. + J_{\Lambda_1}^n(\vec{r}, E) Z_{\Lambda_1}^{n \times}(\vec{r}', E) \Theta(r - r') \right] \delta_{nn'}\end{aligned} \quad (\text{A5})$$

and the perturbation ΔV associated with a change of the spin-dependent potential due to a rotation of the spin magnetic moment, given by the expression

$$\Delta V(r) = V_{\hat{s}}(r) - V_{\hat{s}_0}(r) = \beta(\vec{\sigma} \cdot \delta \hat{s}) B(r), \quad (\text{A6})$$

(where $\delta \hat{s} = (\delta \hat{s}^x, \delta \hat{s}^y, \delta \hat{s}^z)$), one obtains the expression for the exchange coupling parameters as follows

$$\begin{aligned}J_{ij}^{\alpha\beta} &= \frac{\partial^2 \mathcal{F}^{(2)}}{\partial \hat{s}_i^\alpha \partial \hat{s}_j^\beta} \\ &= -\frac{1}{2\pi} \left[\text{ImTr} \int_{E_{\text{bottom}}}^{\infty} dE \frac{df(E)}{dE} (E - E_F) \langle \Delta V \rangle_i^\alpha \tau_{ij}(E) \langle \Delta V \rangle_j^\beta \tau_{ji}(E) \right. \\ &\quad \left. + \text{ImTr} \int_{E_{\text{bottom}}}^{\infty} dE f(E) \langle \Delta V \rangle_i^\alpha \tau_{ij}(E) \langle \Delta V \rangle_j^\beta \tau_{ji}(E) \right],\end{aligned} \quad (\text{A7})$$

where Green function in Eq. (A5) in terms of the wave functions $Z_{\Lambda}^n(\vec{r}, E)$ and $J_{\Lambda}^n(\vec{r}, E)$ and the scattering path operator $\tau_{\Lambda\Lambda'}^{nn'}(E)$ ⁴⁶ was used.

Using naive arguments, the time dependent behavior of $\mathcal{E}^{(2)}$ and as a result of the exchange coupling parameters may be calculated following the scheme used for ground state, but with the Green function $G(E, t)$, calculated for each time step using potentials obtained within the TD-DFT, and using occupation function, $f(E, t)$, calculated for each time step within TD-DFT calculations.

Appendix B: Spin-lattice coupling parameters

Concerning the responsibility of the spin-lattice interactions for the transverse spin excitations, we focus next on the impact of the laser pulse on the behavior of the SLC. The torque on the magnetic moments due to the SLC, $\vec{\mathcal{T}}_i^{SLC} = \hat{s}_i \times \vec{H}_{SLC}$, responsible for the creation of transverse spin fluctuations, may be associated with different types of contributions, e.g. by the MCA-like and DMI-like SLC³⁸. Corresponding effective fields originating from the MCA-like term in the spin-lattice Hamiltonian are given in terms of the parameters $\mathcal{K}_{i,k}^{\alpha z, \mu}$ as follows

$$H_{\text{sl-MA},i}^{\alpha} = \sum_k K_{i,k}^{z\alpha, \mu} (u_k^{\mu} - u_i^{\mu}), \quad (\text{B1})$$

while the DMI-like interactions give rise to the effective field

$$H_{\text{sl-DMI},i}^{\alpha} = \sum_{j,k,\mu} [\hat{s}_j \times \mathcal{D}_{ij,k}^{\mu}]_{\alpha} (u_k^{\mu} - u_i^{\mu}). \quad (\text{B2})$$

On the other hand, the SLC-driven force on atom k due to a spin tilting on site i in the case of MCA-like SLC is given by the expression

$$\mathcal{F}_{\text{sl-MA},k}^{\mu} = \sum_{\alpha} K_{i,k}^{z\alpha, \mu} \delta \hat{s}_i^{\alpha} \quad (\text{B3})$$

and in the case of DMI-like SLC the force looks as follows

$$\mathcal{F}_{\text{sl-DMI},k}^{\mu} = \sum_{j,\alpha} [\hat{s}_j \times \vec{\mathcal{D}}_{ij,k}^{\mu}]_{\alpha} \delta \hat{s}_i^{\alpha}. \quad (\text{B4})$$

Note that the expressions for the SLC parameters $\mathcal{K}_{i,k}^{\alpha z, \mu}$ and $\vec{\mathcal{D}}_{ij,k}^{\mu}$ derived for the ground state^{37,38} should be modified taking into account re-population of the laser-perturbed electronic states, that can be done in line with the corresponding modifications given in the Appendix for isotropic exchange coupling parameters.

-
- ¹ E. Beaurepaire, J.-C. Merle, A. Daunois, and J.-Y. Bigot, *Phys. Rev. Lett.* **76**, 4250 (1996).
- ² A. Kirilyuk, A. V. Kimel, and T. Rasing, *Rev. Mod. Phys.* **82**, 2731 (2010).
- ³ J.-Y. Bigot and M. Vomir, *Annalen der Physik* **525**, 2 (2013), <https://onlinelibrary.wiley.com/doi/pdf/10.1002/andp.201200199>.
- ⁴ K. Carva, P. Baláz, and I. Radu (Elsevier, 2017) pp. 291–463.
- ⁵ J.-Y. Bigot, L. Guidoni, E. Beaurepaire, and P. N. Saeta, *Phys. Rev. Lett.* **93**, 077401 (2004).
- ⁶ M. Fähnle, C. Illg, M. Haag, and N. Teeny, *Acta Phys. Polonica A* **127**, 170 (2015).
- ⁷ B. Koopmans, G. Malinowski, F. Dalla Longa, D. Steiauf, M. Fähnle, T. Roth, M. Cinchetti, and M. Aeschlimann, *Nature Materials* **9**, 259 (2010).
- ⁸ W. Hübner and K. H. Bennemann, *Phys. Rev. B* **53**, 3422 (1996).
- ⁹ C. Dornes, Y. Acremann, M. Savoini, M. Kubli, M. J. Neugebauer, E. Abreu, L. Huber, G. Lantz, C. A. F. Vaz, H. Lemke, E. M. Bothschafter, M. Porer, V. Esposito, L. Rettig, M. Buzzi, A. Alberca, Y. W. Windsor, P. Beaud, U. Staub, D. Zhu, S. Song, J. M. Glowina, and S. L. Johnson, *Nature* **565**, 209 (2019).
- ¹⁰ G. P. Zhang and T. F. George, *Phys. Rev. B* **78**, 052407 (2008).
- ¹¹ G. P. Zhang and W. Hübner, *Phys. Rev. Lett.* **85**, 3025 (2000).
- ¹² K. Carva, M. Battiato, and P. M. Oppeneer, *Phys. Rev. Lett.* **107**, 207201 (2011).
- ¹³ C. Illg, M. Haag, and M. Fähnle, *Phys. Rev. B* **88**, 214404 (2013).
- ¹⁴ K. Carva, M. Battiato, D. Legut, and P. M. Oppeneer, “Theory of femtosecond laser-induced demagnetization,” in *Ultrafast Magnetism I: Proceedings of the International Conference UMC 2013 Strasbourg, France* (Springer International Publishing Switzerland 2015, Cham, Heidelberg, New York, Dordrecht, London, 2015) pp. 111–115.
- ¹⁵ K. Krieger, J. K. Dewhurst, P. Elliott, S. Sharma, and E. K. U. Gross, *ArXiv e-prints*, 1406.6607 (2014), [arXiv:1406.6607 \[cond-mat.mtrl-sci\]](https://arxiv.org/abs/1406.6607).
- ¹⁶ S. Sharma, S. Shallcross, P. Elliott, and J. K. Dewhurst, *Science advances* **8**, eabq2021 (2022).
- ¹⁷ A. J. Schellekens and B. Koopmans, *Phys. Rev. Lett.* **110**, 217204 (2013).
- ¹⁸ M. Fähnle, T. Tsatsoulis, C. Illg, M. Haag, B. Y. Müller, and L. Zhang, *Journal of Superconductivity and Novel Magnetism* **30**, 1381 (2017).
- ¹⁹ S. Eich, M. Plötzing, M. Rollinger, S. Emmerich, R. Adam, C. Chen, H. C. Kapteyn, M. M. Murnane, L. Plucinski, D. Steil, B. Stadtmüller, M. Cinchetti, M. Aeschlimann, C. M. Schneider, and S. Mathias, *Science Advances* **3** (2017), 10.1126/sciadv.1602094, <http://advances.sciencemag.org/content/3/3/e1602094.full.pdf>.
- ²⁰ P. Tengdin, W. You, C. Chen, X. Shi, D. Zusin, Y. Zhang, C. Gentry, A. Blonsky, M. Keller, P. M. Oppeneer, H. C. Kapteyn, Z. Tao, and M. M. Murnane, *Science Advances* **4**, eaap9744 (2018),

- <https://www.science.org/doi/pdf/10.1126/sciadv.aap9744>.
- ²¹ N. Kazantseva, U. Nowak, R. W. Chantrell, J. Hohlfeld, and A. Rebei, *Europhysics Letters* **81**, 27004 (2007).
 - ²² A. Deák, D. Hinzke, L. Szunyogh, and U. Nowak, *Journal of Physics: Condensed Matter* **29**, 314003 (2017).
 - ²³ M. Weißenhofer and M. P. Oppeneer, arXiv , 2309.14167v3 (2023).
 - ²⁴ P. Němec, E. Rozkotová, N. Tesařová, F. Trojánek, E. De Ranieri, K. Olejník, J. Zemen, V. Novák, M. Cukr, P. Malý, and T. Jungwirth, *Nature Physics* **8**, 411 (2012).
 - ²⁵ R. R. Subkhangulov, A. B. Henriques, P. H. O. Rappl, E. Abramof, T. Rasing, and A. V. Kimel, *Scientific Reports* **4**, 4368 (2014).
 - ²⁶ R. V. Mikhaylovskiy, E. Hendry, A. Secchi, J. H. Mentink, M. Eckstein, A. Wu, R. V. Pisarev, V. V. Kruglyak, M. I. Katsnelson, T. Rasing, and A. V. Kimel, *Nature Communications* **6**, 8190 (2015).
 - ²⁷ F. Freimuth, S. Blügel, and Y. Mokrousov, *Phys. Rev. B* **94**, 144432 (2016).
 - ²⁸ J. H. Mentink, *Journal of Physics: Condensed Matter* **29**, 453001 (2017).
 - ²⁹ H. Hamamera, F. S. M. Guimarães, M. dos Santos Dias, and S. Lounis, *Communications Physics* **5**, 16 (2022).
 - ³⁰ A. S. Núñez, J. Fernández-Rossier, M. Abolfath, and A. MacDonald, *Journal of Magnetism and Magnetic Materials* **272-276**, 1913 (2004), proceedings of the International Conference on Magnetism (ICM 2003).
 - ³¹ A. Rückriegel, S. Streib, G. E. W. Bauer, and R. A. Duine, *Phys. Rev. B* **101**, 104402 (2020).
 - ³² B. Frietsch, A. Donges, R. Carley, M. Teichmann, J. Bowlan, K. Döbrich, K. Carva, D. Legut, P. M. Oppeneer, U. Nowak, and M. Weinelt, *Science Advances* **6**, eabb1601 (2020), <https://www.science.org/doi/pdf/10.1126/sciadv.abb1601>.
 - ³³ M. van Kampen, C. Jozsa, J. T. Kohlhepp, P. LeClair, L. Lagae, W. J. M. de Jonge, and B. Koopmans, *Phys. Rev. Lett.* **88**, 227201 (2002).
 - ³⁴ A. Secchi, S. Brener, A. Lichtenstein, and M. Katsnelson, *Annals of Physics* **333**, 221 (2013).
 - ³⁵ W. Hübner and G. P. Zhang, *Phys. Rev. B* **58**, R5920 (1998).
 - ³⁶ S. Bhattacharjee, L. Nordström, and J. Fransson, *Phys. Rev. Lett.* **108**, 057204 (2012).
 - ³⁷ S. Mankovsky, S. Polesya, H. Lange, M. Weißenhofer, U. Nowak, and H. Ebert, *Phys. Rev. Lett.* **129**, 067202 (2022).
 - ³⁸ S. Mankovsky, H. Lange, S. Polesya, and H. Ebert, *Phys. Rev. B* **107**, 144428 (2023).
 - ³⁹ “The Elk Code,” <http://elk.sourceforge.net/>.
 - ⁴⁰ A. I. Liechtenstein, M. I. Katsnelson, V. P. Antropov, and V. A. Gubanov, *J. Magn. Magn. Materials* **67**, 65 (1987).
 - ⁴¹ L. Udvardi, L. Szunyogh, K. Palotás, and P. Weinberger, *Phys. Rev. B* **68**, 104436 (2003).
 - ⁴² H. Ebert and S. Mankovsky, *Phys. Rev. B* **79**, 045209 (2009).
 - ⁴³ S. Mankovsky, S. Polesya, and H. Ebert, *Phys. Rev. B* **101**, 174401 (2020).
 - ⁴⁴ J. B. Staunton, L. Szunyogh, A. Buruzs, B. L. Gyorffy, S. Ostanin, and L. Udvardi, *Phys. Rev. B* **74**, 144411 (2006).
 - ⁴⁵ H. Ebert, S. Mankovsky, K. Chadova, S. Polesya, J. Minár, and D. Ködderitzsch, *Phys. Rev. B* **91**, 165132 (2015).
 - ⁴⁶ H. Ebert, J. Braun, D. Ködderitzsch, and S. Mankovsky, *Phys. Rev. B* **93**, 075145 (2016).